

Driving Force of Ultrafast Magnetization Dynamics

B. Y. Mueller, T. Roth, M. Cinchetti, M. Aeschlimann, B. Rethfeld

Department of Physics and Research Center OPTIMAS, Technical University of Kaiserslautern, Erwin-Schrödinger-Str. 46, 67653 Kaiserslautern, Germany

E-mail: bmueeller@physik.uni-kl.de

Abstract. Irradiating a ferromagnetic material with an ultrashort laser pulse leads to demagnetization on a femtosecond timescale. We implement Elliott-Yafet type spin-flip scattering, mediated by electron-electron and electron-phonon collisions, into the framework of a spin-resolved Boltzmann equation. Considering three mutually coupled reservoirs, (i) spin-up electrons, (ii) spin-down electrons and (iii) phonons, we trace non-equilibrium electron distributions during and after laser excitation. We identify the driving force for ultrafast magnetization dynamics as the equilibration of temperatures and chemical potentials between the electronic subsystems. This principle can be used to easily predict the maximum quenching of magnetization upon ultrashort laser irradiation in any material, as we show for the example of 3d-ferromagnetic nickel.

Interaction of a femtosecond laser pulse with ferromagnetic metal is known for more than a decade to cause ultrafast quenching of the magnetization [1]. Typical demagnetization times extracted from experiments on the 3d-ferromagnetic metals Co, Fe and Ni are between 100 fs and 300 fs, depending on the laser fluence and the specific sample [2, 3, 4, 5]. From the theoretical side, intense efforts are being undertaken in order to identify the microscopic mechanisms responsible for the observed behavior [6, 7, 8, 9, 10, 11, 12, 13, 14, 15]. Among the considered mechanisms, Elliott-Yafet (EY)-type spin-flip scattering [16] is definitely one of the most implemented for the modeling of ultrafast demagnetization. The most popular EY-type spin-flip mechanism is electron-phonon (el-ph) scattering [2, 10, 13, 14, 15], while recently electron-electron (el-el) Coulomb scattering has been considered as well [11, 17]. Based on EY-type el-ph scattering, Koopmans et al. developed the so-called Microscopic Three-Temperature Model (M3TM), which has been shown to possess a great predictive power, explaining not only the demagnetization in ferromagnetic transition metals but also the specific demagnetization characteristics of gadolinium [2]. Electron-electron Coulomb scattering has been implemented in a dynamical model including momentum- and spin-dependent carrier scattering [11], in the following referred to as the el-el Coulomb (EEC) model. Since the band structure is taken as input for the calculations, the EEC model can be successfully applied to understand the demagnetization dynamics in materials with peculiar band structure, as recently shown for the case of half-metallic Heusler alloys [17].

However, a fundamental question remains still unsolved: What is the ultimate “driving force” for ultrafast demagnetization?

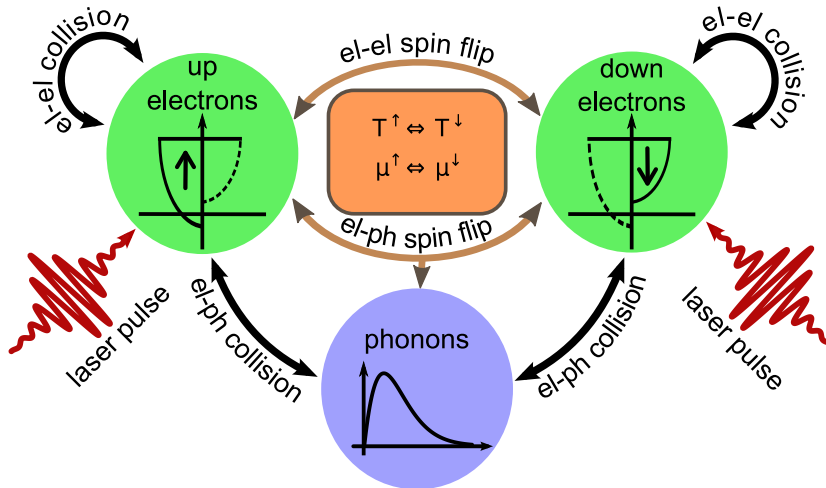


Figure 1. Scheme of the spin-resolved Boltzmann equation: It separates the phononic and the electronic system, the latter subdivided into a majority and a minority part. Due to the spin-mixing, both electronic systems are coupled by electron-electron and electron-phonon spin-flips. In its essence, the driving force for the ultrafast demagnetization is determined by an equilibration of temperatures and chemical potentials between the two electronic systems.

To answer this question, we introduce a simplified, yet microscopic kinetic model, describing non-equilibrium electron dynamics in laser-excited ferromagnetic metals. It combines the basic ingredients of the M3TM and the EEC model in the framework of a *spin-resolved Boltzmann equation*. The main idea behind this approach is schematically depicted in Fig. 1. Based on the EEC model, we describe a ferromagnetic metal as consisting of three subsystems: the spin-up (majority) electrons, the spin-down (minority) electrons, and the phonon system. We consider el-el spin-flips and additionally, in the spirit of the M3TM, we include el-ph mediated spin-flips but without the need of introducing a separate spin subsystem. In order to enable the implementation of complete Boltzmann collision integrals and to ensure a clear interpretation of the results it is necessary to make simplifying assumptions, like the free electron gas density of states (DOS) for the two spin subsystems. The strength of our approach is that it allows to assign a respective temperature and chemical potential to up and down electrons, denoted by $T^{\uparrow,\downarrow}$ and $\mu^{\uparrow,\downarrow}$. We find that the equilibration of these quantities is the driving force of ultrafast demagnetization. This equilibration condition can be easily applied to real materials with complex DOS to obtain the maximum magnetization quenching following laser excitation, as we exemplarily show for nickel. As a further result, our approach is capable to clarify the relative role played by el-el and el-ph scattering during ultrafast demagnetization.

In our model, we calculate the time- and energy dependent dynamics of the considered subsystems on the basis of a kinetic approach applying complete Boltzmann collision integrals [18]. The interactions between electrons (el-el), electrons and phonons (el-ph) as well as the absorption of laser energy (absorp) are described as independent collision integrals Γ_{col} , respectively. Their sum yields the transient evolutions of the electronic distribution $f(E)$ and the phononic distribution $g(E)$. The particular collision integrals are generally derived by Fermi's golden rule

$$\Gamma_{\text{col}} = \sum_{\text{all states}} \frac{2\pi}{\hbar} |\langle \varphi_0 | \hat{H}_{\text{col}} | \varphi_1 \rangle|^2 \delta(E_0 - E_1) , \quad (1)$$

where \hat{H}_{col} indicates the Hamiltonian for the considered collision process, φ_0 the initial state with energy E_0 and φ_1 the final state with energy E_1 . Such model was developed in Ref. [18] to describe non-equilibrium electron and phonon dynamics during and after ultrafast laser excitation for a non-magnetic material. It is capable to account for non-equilibrium distribution functions where no real temperatures are defined.

First, to apply this approach to ferromagnetic metals we include the Stoner model into the existing theory. This leads to a separated description of the two spin systems (up and down electrons), with a constant energy shift by the exchange energy Δ_{ex} between the corresponding distribution functions.

Second, we include spin-mixing in our approach. This allows a coupling between both electronic reservoirs: Typically, the orthogonality of the up and down states guarantees that the matrix element $\langle \uparrow | \downarrow \rangle$ vanishes and for a spin diagonal interaction operator, there will be no possibility for an electron to change its spin during a collision

process. But due to the spin orbit coupling in solids, no pure up or down states are defined, but a mixture of both [13, 14]. In this case, an up-electron, for instance, is described by the state

$$|\tilde{\uparrow}\rangle = a |\uparrow\rangle + b |\downarrow\rangle , \quad (2)$$

whereby $|b| \ll |a|$. As the matrix element of the mixed state is larger than zero ($|\langle\tilde{\uparrow}|\tilde{\downarrow}\rangle| > 0$), the spin orbit coupling allows for spin-flip and thus induces an interaction between the two spin systems in our model. The collisions including the spin-mixing are thus described by

$$\begin{aligned} \tilde{\Gamma}_{\text{col}} &= \sum_{\text{all states}} \frac{2\pi}{\hbar} |\langle\sigma_0|\langle\varphi_0|\hat{H}_{\text{col}}|\varphi_1\rangle|\sigma_1\rangle|^2 \delta(E_0 - E_1) \\ &= |\langle\sigma_0|\sigma_1\rangle|^2 \sum_{\text{all states}} \frac{2\pi}{\hbar} \langle\varphi_0|\hat{H}_{\text{col}}|\varphi_1\rangle|^2 \delta(E_0 - E_1) \\ &\equiv |\langle\sigma_0|\sigma_1\rangle|^2 \Gamma_{\text{col}} , \end{aligned} \quad (3)$$

whereby φ_i is the spatial and $\sigma_i \in \{\tilde{\uparrow}, \tilde{\downarrow}\}$ the (mixed) spin wave function of the electron.

With all the described ingredients, we can now write down the *spin-resolved Boltzmann equation*

$$\begin{aligned} \frac{\partial f^\mu}{\partial t} &= \sum_{\sigma, \nu, \lambda} |\langle\mu, \sigma|\nu, \lambda\rangle|^2 \Gamma_{\text{el-el}} \\ &+ \sum_{\sigma} |\langle\mu|\sigma\rangle|^2 \Gamma_{\text{el-ph}} + \sum_{\sigma} |\langle\mu|\sigma\rangle|^2 \Gamma_{\text{absorp}} \end{aligned} \quad (4a)$$

$$\frac{\partial g}{\partial t} = \sum_{\mu, \sigma} |\langle\mu|\sigma\rangle|^2 \Gamma_{\text{ph-el}} , \quad (4b)$$

with $\mu, \nu, \sigma, \lambda \in \{\tilde{\uparrow}, \tilde{\downarrow}\}$ indicating the spin states. Eq. (4) consists of three equations for f^\uparrow , f^\downarrow and g , respectively. The collision terms Γ_{col} can be found in Refs. [18, 19]. Each of the distinct equations is coupled to both others, thus the dynamics of all three subsystems mutually depend on each other. Since the description allows for spin-flips, the number of particles in each electronic reservoir is not conserved. Instead, the *sum* of the transient number of particles of spin-up (n^\uparrow) and spin-down (n^\downarrow) is conserved. The transient magnetization M is calculated through

$$M(t) = \mu_B(n^\uparrow(t) - n^\downarrow(t)) = \mu_B \Delta n(t) , \quad (5)$$

whereby μ_B is the Bohr magneton.

We solve the spin-resolved Boltzmann equation (4) for a prototype of a ferromagnetic material with the Fermi energy $E_F = 8$ eV, the effective mass $m^* = 1.45 m_e$ and the density of states of a free electron gas. We assume the exchange energy $\Delta_{\text{ex}} = 2$ eV. The spin-mixing parameter $b^2 \approx 0.03$ in Eq. (2) is chosen according to ab initio calculations for Ni [2, 13, 14]. For the phononic system we apply the Debye model with $T_D = 724$ K as Debye temperature. These parameters represent typical

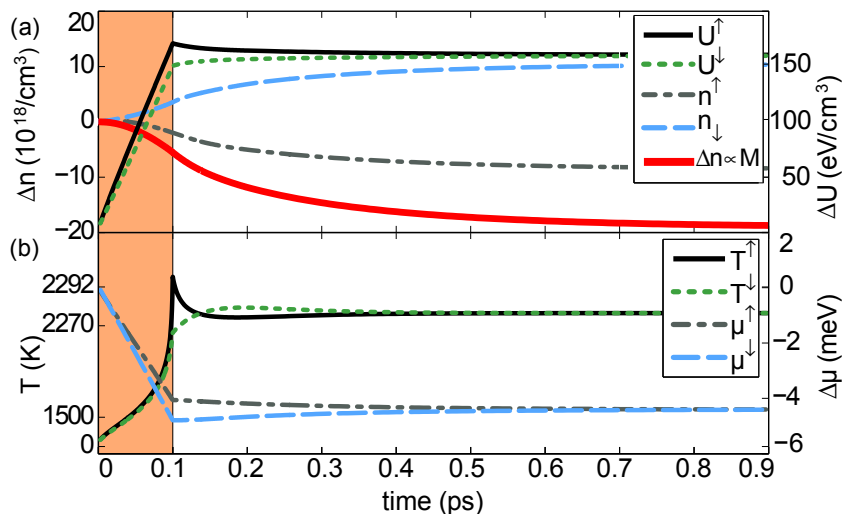


Figure 2. Simulation neglecting the contribution of phonons. (a) The internal energy $U^{\uparrow,\downarrow}$ and number of particles $n^{\uparrow,\downarrow}$ of each electronic system. (b) Applying Eq. (8) it is possible to define approximated temperatures $T^{\uparrow,\downarrow}$ and chemical potentials $\mu^{\uparrow,\downarrow}$. The chemical potentials and the corresponding temperatures approach each other asymptotically.

values for real metals. Note that none of them is used as a fit parameter, because it is not in the scope of this article to reproduce the experimental data, but to identify the driving force of ultrafast demagnetization. In this spirit we chose the density of states of a free electron gas because essential relations are given analytically and the solution of the spin-resolved Boltzmann equation can thus be easily interpreted. Finally, to clearly investigate the processes after optical excitation, we assume a rectangular laser profile in time.

In order to solve the spin-resolved Boltzmann equation (4) we compute a system of approximately 300 strongly coupled integro-differential equations. The solution provides the transient non-equilibrium distribution function of each electronic reservoir. It resembles the evolution of the electron distribution in Fig. 1 of Ref. [18], but extended by the information on the two spin reservoirs. In particular, a net spin-flip is observed as a slight particle exchange between both electron reservoirs in the solution of Eq. (4) during and after irradiation. Figures 2 and 3 were calculated for a 100 fs laser pulse with wavelength $\lambda = 630$ nm and a total absorbed fluence of $F = 0.13$ mJ/cm². In Fig. 3, which will be discussed later in detail, curve (a) shows the transient magnetization (normalized to the initial magnetization) obtained with the spin-resolved Boltzmann equation (4) and applying Eq. (5). We obtain a demagnetization time of $\tau_M \approx 100$ fs after laser irradiation. Remagnetization occurs on a picosecond timescale.

Generally, when a system is excited out of its equilibrium state, it tends back to a new equilibrium. An example is the relaxation between electrons and phonons after ultrafast laser excitation. Here, the initially heated electrons transfer energy to the lattice in a way that both end at a new, higher temperature. The nonequilibrium

of temperatures between both systems drives this energy exchange. However, what is the driving force of particle exchange between spin-up and spin-down electrons, which, according to Eq. (5), is the basis for magnetization dynamics? For such a system, allowing for energy *and* particle exchange, the equilibrium condition refers to temperature *and* chemical potential and reads

$$T^\uparrow = T^\downarrow \quad \text{and} \quad \mu^\uparrow = \mu^\downarrow + \Delta_{\text{ex}} . \quad (6)$$

Exploiting the simplifications possible for a free electron gas, the chemical potentials can be explicitly expressed by the Sommerfeld expansion:

$$\mu^{\uparrow,\downarrow}(T^{\uparrow,\downarrow}) = E_F(n^{\uparrow,\downarrow}) \left[1 - \frac{\pi^2}{12} \left(\frac{k_B T^{\uparrow,\downarrow}}{E_F(n^{\uparrow,\downarrow})} \right)^2 + \dots \right] . \quad (7)$$

After optical excitation, the temperatures T^\uparrow and T^\downarrow will be increased. Let us assume that T^\uparrow and T^\downarrow were already equalized. Then Eq. (7) clarifies that in order to equal also the chemical potentials μ^\uparrow and μ^\downarrow , a change of $E_F(n^{\uparrow,\downarrow})$, mediated by a change of n^\uparrow and n^\downarrow , is required. Thus, it is the equilibration of chemical potentials of the two electronic subsystems, which leads to a particle exchange between both reservoirs and thus provides the ultimate driving force for ultrafast magnetization dynamics.

Our model allows to verify the conclusion of the driving force behind the demagnetization process because we can selectively suppress different scattering channels in Eq. (4). In the following, we discard the phononic influence by setting $\Gamma_{\text{el-ph}} = \Gamma_{\text{ph-el}} = 0$. The transient spin-resolved density $n^{\uparrow,\downarrow}$ and internal energy $U^{\uparrow,\downarrow}$ are depicted in dependence on time in Fig. 2(a) together with the difference Δn , being proportional to the magnetization. Due to the higher electron density of majority electrons the amount of energy absorbed by the spin-up electrons is larger than for the spin-down electrons. For each moment in time and both spin directions we may define a temperature $T^{\uparrow,\downarrow}$ and a chemical potential $\mu^{\uparrow,\downarrow}$ of the current distribution function. Both quantities are found through the implicit integral equations of the corresponding Fermi distribution f_F :

$$n^{\uparrow,\downarrow}(t) \stackrel{!}{=} \int f_F^{\uparrow,\downarrow}(E, T^{\uparrow,\downarrow}, \mu^{\uparrow,\downarrow}) \text{DOS}(E) dE , \quad (8a)$$

$$U^{\uparrow,\downarrow}(t) \stackrel{!}{=} \int f_F^{\uparrow,\downarrow}(E, T^{\uparrow,\downarrow}, \mu^{\uparrow,\downarrow}) \text{DOS}(E) E dE . \quad (8b)$$

The resulting temperatures $T^{\uparrow,\downarrow}$ and chemical potentials $\mu^{\uparrow,\downarrow}$ are depicted in Fig. 2(b). Due to laser excitation, both temperatures increase, while the chemical potentials drop. When the laser is turned off (at $t = 100$ fs) the two spin systems differ in temperatures *and* chemical potentials. Since this difference is small for the assumed case of free electron like density of states (second order term in Eq. (7)), the quenching of magnetization is also considerably lower than observed in real materials. Subsequently, the reservoirs equilibrate until a same temperature T *and* chemical potential μ are

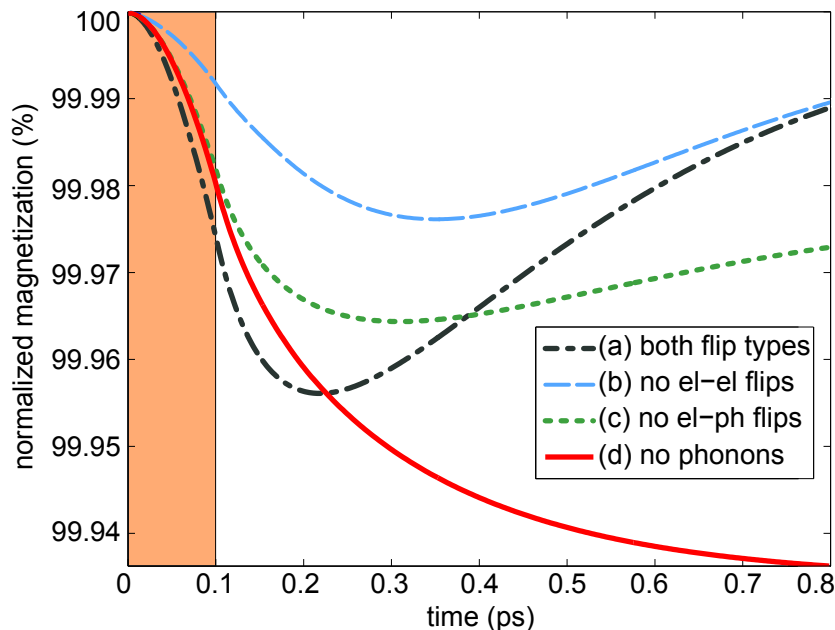


Figure 3. Magnetization dynamics regarding the different scattering processes separately. The calculations were performed by applying the spin-resolved Boltzmann equation for a free electron gas.

reached. According to Eq. (6) *both* constraints have to be satisfied to reach an equilibrium between the electronic systems. Fig. 2 (b) verifies that the temperatures and chemical potentials equilibrate simultaneously. Comparing with Fig. 2 (a), we find that also the transient magnetization, being proportional to Δn , reaches its asymptotical value on the same timescale. In its essence, the particle exchange affected by the difference in chemical potentials provides the driving force for ultrafast magnetization.

In order to estimate the effect for more realistic systems, we choose nickel and solve the equilibrium condition (6) applying the implicit equations (8) with the real density of states for Ni [20]. Note that this can be done without explicitly solving the spin-resolved Boltzmann equation. In case of starting at room temperature and ending up at an electron temperature of $T_e \equiv T^\uparrow = T^\downarrow = 3000$ K a maximum quenching of 30% is found. Such transient electron temperatures are typical for ultrafast laser excitation of metals below melting threshold [18, 21]. Thus, applying the main result of our simplified model to realistic systems leads to quantitative agreement with experiments, demonstrating the solidity of our findings.

To show the great potential of the spin-resolved Boltzmann equation, we now exemplarily compare the relative effects of el-el spin-flips and el-ph spin-flips on the demagnetization process. We again restrict ourselves to the case of a free electron gas. Figure 3 represents the calculated magnetization dynamics obtained with the spin-resolved Boltzmann equation (4), when different collision processes are regarded separately. The red solid line (d) corresponds to the red solid line in Fig. 2 (a), determining the magnetization dynamics when the influence of the phonon bath is

completely discarded. Including the cooling by phonons but disregarding el-ph spin-flips (green dotted line (c)), we see a slight recovery of magnetization.

Thus, phonon cooling is essential for the *remagnetization* process. However, phonons also strengthen the magnetization dynamics: If we additionally allow for phonon mediated spin-flips we find the black dash-dotted curve (a). The demagnetization occurs faster than in the case where only electron collisions mediate spin-flips, while the remagnetization is strongly accelerated by phonon mediated spin-flips. Hence, phonons can act like a catalyst for the ultrafast magnetization process. The blue dashed line (b) is calculated excluding electron-electron-collision mediated spin-flips. In this case, the quenching of magnetization will be less. Comparing the simulations shown in Fig. 3 we conclude that for our system electron mediated spin-flips are important mainly during the *demagnetization* phase, while phonon mediated spin-flips dominate the *remagnetization* phase and increase the effectiveness of the demagnetization.

In conclusion, we described the ultrafast demagnetization with the spin-resolved Boltzmann equation. We identified the driving force of the demagnetization process in the equilibration of the temperatures *and* chemical potentials of the up and down electrons. As shown for the example of Ni this equilibrium condition provides a possibility to easily estimate the maximum quenching for any ferromagnetic material. Our approach is also capable to investigate the role of different scattering processes during ultrafast demagnetization dynamics.

Acknowledgement

We acknowledge fruitful discussions with H. C. Schneider. Financial support of the Network Project "UltraMagnetron" of the European Union and the Deutsche Forschungsgemeinschaft through the GRK 792 "Nonlinear Optics and Ultrafast Dynamics" and the Emmy Noether project RE 1141/11-1 "Ultrafast Dynamics of laser-excited Solids" is gratefully acknowledged.

References

- [1] E. Beaurepaire, J.-C. Merle, A. Daunois, and J.-Y. Bigot *Phys. Rev. Lett.* **76**, 4250 (1996)
- [2] B. Koopmans, F. Dalla Longa, G. Malinowski, D. Steiauf, M. Fähnle, T. Roth, M. Cinchetti, and M. Aeschlimann, *Nature Materials* **9**, 259-265 (2010)
- [3] C. Stamm, T. Kachel, N. Pontius, R. Mitzner, T. Quast, K. Holldack, S. Khan, C. Lupulescu, E. F. Aziz, M. Wietstruk, H. Durr, W. Eberhardt *Nature Materials* **6**, 740-743 (2007)
- [4] M. Cinchetti, M. Sánchez Albaneda, D. Hoffmann, T. Roth, J.-P. Wüstenberg, M. Krauß, O. Andreyev, H. C. Schneider, M. Bauer and M. Aeschlimann *Phys. Rev. Lett* **97**, 177201 (2006)
- [5] G. Müller, G. Eilers, Z. Wang, M. Scherff, R. Ji, K. Nielsch, C. Ross and M. Münzenberg *New J. Phys.* **10**, 123004 (2008)
- [6] J.-Y. Bigot, M. Vomir, E. Beaurepaire, *Nature Physics* **5**, 515 (2009)
- [7] E. Carpene, E. Mancini, C. Dallera, M. Brenna, E. Puppini, S. De Silvestri *Phys. Rev. B* **78**, 174422 (2008)
- [8] G. P. Zhang, W. Hübner, *Phys. Rev. Lett.* **85**, 3025 (2000).

- [9] N. Kazantseva, U. Nowak, R. W. Chantrell, J. Hohlfeld and A. Rebei *Europhys. Lett.* **81**, 27004 (2008)
- [10] B. Koopmans, J. J. M. Ruigrok, F. Dalla Longa, and W. J. M. de Jonge *Phys. Rev. Lett.* **95**, 267207 (2005)
- [11] M. Krauss, T. Roth, S. Alebrand, D. Steil, M. Cinchetti, M. Aeschlimann, H. C. Schneider, *Phys. Rev. B* **80**, 180407(R) (2009)
- [12] M. Battiato, K. Carva, P. M. Oppeneer, *Phys. Rev. Lett.* **105**, 027203 (2010)
- [13] D. Steiauf and M. Fähnle, *Phys. Rev. B* **79**, 140401(R) (2009)
- [14] D. Steiauf, C. Illg and M. Fähnle, *J. of Phys.: Conference Series* **200**, 042024 (2010)
- [15] M. Fähnle, J. Seib and C. Illg, *Phys. Rev. B* **82**, 144405 (2010)
- [16] I. Žutić, J. Fabian, and S. Das Sarma, *Rev. Mod. Phys.* **76**, 323 (2004).
- [17] D. Steil, S. Alebrand, T. Roth, M. Krauß, T. Kubota, M. Oogane, Y. Ando, H. C. Schneider, M. Aeschlimann and M. Cinchetti *Phys Rev. Lett.* **105**, 217202 (2010)
- [18] B. Rethfeld, A. Kaiser, M. Vicanek and G. Simon, *Phys. Rev. B* **65**, 214303 (2002)
- [19] A. Kaiser, B. Rethfeld, M. Vicanek, G. Simon *Phys. Rev. B* **61** 11437 (2000)
- [20] Z. Lin, L. V. Zhigilei and V. Celli, *Phys. Rev. B* **77**, 075133 (2008)
- [21] D. S. Ivanov, B. Rethfeld, *Appl. Surf. Science* **255**, 9724 (2009)